

Effect of SUSY-QCD corrections to neutralino annihilation on the cold dark matter relic density in the Higgs funnel

Björn Herrmann

Laboratoire de Physique Subatomique et de Cosmologie
 Université Joseph Fourier / CNRS-IN2P3 / INPG, 53 Avenue des Martyrs, 38026 Grenoble, France

September 5, 2007

Abstract. We present a complete calculation of the QCD and SUSY-QCD corrections to neutralino pair annihilation into bottom quark-antiquark pairs through exchange of a pseudoscalar Higgs boson, which is the dominant process in the cosmological *A-funnel* region of the mSUGRA model. We present numerical predictions for the annihilation cross section and discuss the influence of the correction terms on the cold dark matter relic density with respect to recent cosmological data.

PACS. 12.38.Cy Summation of perturbation theory – 12.60.Jv Supersymmetric models – 95.30.Cq Elementary particle processes – 95.35.+d Dark matter (stellar, interstellar, galactic, and cosmological)

1 Motivation

Thanks to the recent WMAP mission and further cosmological observations, the matter and energy decomposition of our Universe is known today with unprecedented precision [1]. Direct evidence for the existence of Cold Dark Matter (CDM) is accumulating [2], and its relic density Ω_{CDM} can be constrained to rather narrow range [3]

$$0.094 \leq \Omega_{\text{CDM}} h^2 \leq 0.136 \quad (1)$$

at 95% confidence level. h denotes the present Hubble expansion rate H_0 in units of $100 \text{ km s}^{-1} \text{ Mpc}^{-1}$.

Although the nature of dark matter remains still unknown, extensions of the Standard Model (SM) of particle physics provide interesting candidates for these Weakly Interacting Massive Particles (WIMPs). In Supersymmetry (SUSY), a natural candidate is the Lightest Supersymmetric Particle (LSP), which is stable, if R -parity is conserved. It is usually the lightest of the four neutralinos, denoted $\tilde{\chi}_1^0$ or shortly χ .

The Minimal Supersymmetric SM (MSSM) is governed by 124 a priori free soft SUSY-breaking parameters, which are often restricted to five universal parameters that are imposed at the unification scale and can be constrained using data from high-energy colliders. As the neutralino relic density also depends on these parameters, its computation is another powerful tool to put constraints on the parameter space and provide complementary information, in particular at high energies and masses that would otherwise not be accessible at colliders.

To evaluate the number density n of the relic particle, one has to solve the Boltzmann equation

$$\frac{dn}{dt} = -3Hn - \langle \sigma_{\text{eff}} v \rangle (n^2 - n_{\text{eq}}^2) \quad (2)$$

with the Hubble rate H and the thermal equilibrium density n_{eq} . The number density n is directly related to the relic density $\Omega_{\text{CDM}} h^2 = m_\chi n / \rho_c \propto \langle \sigma_{\text{eff}} v \rangle^{-1}$, where m_χ is the LSP mass, $\rho_c = 3H_0^2 / (8\pi G_N)$ is the critical density of our Universe, and G_N is the gravitational constant [4]. The effective cross section σ_{eff} involves all (co)annihilation processes of the relic particle χ into SM particles, and $\langle \sigma_{\text{eff}} v \rangle$ signifies the thermal average of its non-relativistic expansion ($v \ll c$).

Several public codes perform a calculation of the dark matter relic density within supersymmetric models. The most developed and most popular ones are **DarkSUSY** [6] and **micrOMEGAs** [7]. All relevant (co)annihilation processes are implemented in these codes, but for most of them no (or at least not the complete) higher order corrections are included. However, due to the large magnitude of the strong coupling constant, QCD and SUSY-QCD corrections are bound to affect the annihilation cross section in a significant way. They may even be enhanced logarithmically by kinematics or in certain regions of the parameter space.

It is the aim of this work to study these corrections for the neutralino-pair annihilation into a bottom quark-antiquark pair through exchange of a pseudoscalar Higgs boson A^0 . This process dominates in the so-called *A-funnel* region of the mSUGRA parameter space at large $\tan \beta$, which is theoretically favoured by the unification of Yukawa couplings in Grand Unification Theories (GUTs) [8]. Supposing a WIMP mass

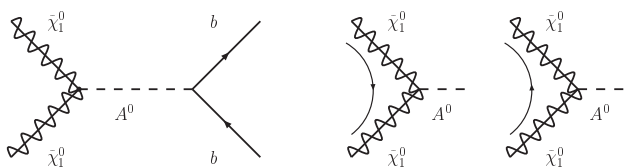


Fig. 1. The tree level diagram for the process $\chi\chi \rightarrow A^0 \rightarrow b\bar{b}$, indicating the two possible fermionic orientations of the Majorana initial state.

of 50 - 70 GeV, this process has been claimed to be compatible with the gamma-ray excess observed by the EGRET satellite in all sky directions [9]. However, the corresponding scenarios may lead to antiproton overproduction, so that they would not be compatible with the observed antiproton flux [10].

2 Analytical results

As we focus here on the phenomenological aspects of this work, the analytical calculation is only briefly sketched. For a more detailed discussion we refer the reader to Ref. [11].

In the calculation of the leading order (LO) amplitude, we have to make sure to anti-symmetrize the neutralino pair in the initial state properly by taking into account both possible fermionic orientations shown on the right-hand side of Fig. 2, leading to a factor $\sqrt{2}$ in the amplitude with respect to the amplitude of one fixed orientation. Denoting by \sqrt{s} the centre-of-momentum energy and $\beta_\chi = v/2$ and β_b the neutralino and b -quark velocities, the leading order cross section can then be written as

$$\sigma_{\text{LO}} v = \frac{1}{2} \frac{\beta_b}{8\pi s} \frac{N_C g^2 T_{A11}^2 h_{Abb}^2 s^2}{|s - m_A^2 + im_A \Gamma_A|^2}. \quad (3)$$

It is proportional to the inverse of the flux factor sv , the integrated two-particle phase space $s\beta_b/(8\pi s)$, the number of quark colours $N_C = 3$ and the squares of the weak coupling constant g , a neutralino mixing factor

$$T_{Aij} = \frac{1}{2} (N_{2j} - \tan \theta_W N_{1j}) (N_{4i} \cos \beta - N_{3i} \sin \beta) + (i \leftrightarrow j), \quad (4)$$

the bottom quark mass through the Yukawa coupling $h_{Abb} = -gm_b \tan \beta / (2m_W)$, and the Higgs boson propagator. The N_{ij} in Eq. (4) are the entries of the matrix N that diagonalizes the neutralino mass matrix. The non-relativistic expansion of Eq. (4) is performed by expanding the squared centre-of-momentum energy s in powers of v^2 ,

$$s \doteq 4m_\chi^2 \left(1 + \frac{v^2}{4} \right) + \mathcal{O}(v^4) \quad (5)$$

and is in agreement with the results given in Ref. [5].

The next-to-leading order (NLO) annihilation cross section can be written as

$$\sigma_{\text{NLO}} = \sigma_{\text{LO}} (1 + \Delta_{\text{QCD}} + \Delta_{\text{top}} + \Delta_{\text{SUSY}}), \quad (6)$$

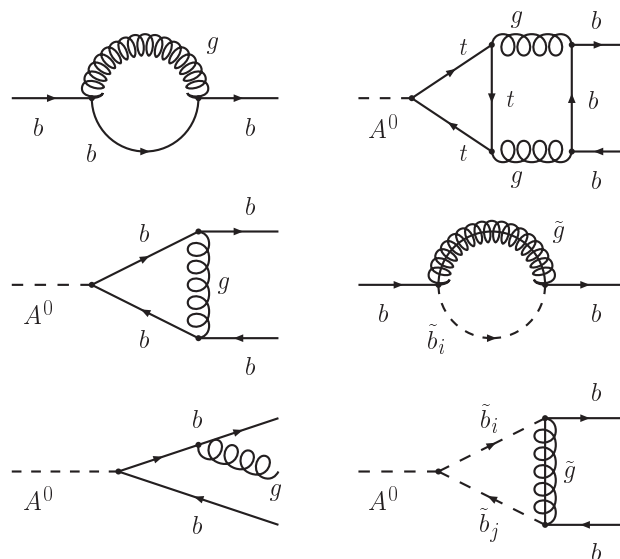


Fig. 2. QCD (left), top-quark loop (right top), and SUSY-QCD (right centre and bottom) correction diagrams for the annihilation process $\chi\chi \rightarrow A^0 \rightarrow b\bar{b}$.

where Δ_{QCD} , Δ_{top} and Δ_{SUSY} relate to the QCD, top-quark loop, and SUSY-QCD correction diagrams shown in Fig. 2. The same relation also holds for the Higgs boson width Γ_A , for which the same correction diagrams are involved. Using standard methods, we compute the QCD correction Δ_{QCD} at $\mathcal{O}(\alpha_s)$, coming from the gluon exchange and real emission diagrams, which agrees with the known result for pseudoscalar Higgs boson decays in the on-shell scheme [12]. In the limit $m_b^2 \ll s$, this correction develops a logarithmic mass singularity, which can be resummed to all orders using the renormalization group, i.e. replacing m_b with the running mass $\bar{m}_b(s)$ in the Yukawa coupling h_{Abb} [13]. The remaining finite QCD corrections in the $\overline{\text{MS}}$ scheme are known up to $\mathcal{O}(\alpha_s^3)$,

$$\Delta_{\text{QCD}} = \frac{\alpha_s(s) C_F}{\pi} \frac{17}{4} + \frac{\alpha_s(s)^2}{\pi^2} (35.94 - 1.36n_f) + \frac{\alpha_s(s)^3}{\pi^3} (164.14 - 25.77n_f + 0.259n_f^2), \quad (7)$$

where n_f denotes the number of flavours [14].

A separately gauge-independent correction at order $\mathcal{O}(\alpha_s^2)$ is induced by the top-quark loop diagram shown in Fig. 2. Its contribution [15]

$$\Delta_{\text{top}} = \frac{1}{\tan^2 \beta} \frac{\alpha_s^2(s)}{\pi^2} \left[\frac{23}{6} - \log \frac{s}{m_t^2} + \frac{1}{6} \log^2 \frac{\bar{m}_b^2}{s} \right] \quad (8)$$

can be important at small values of $\tan \beta$. However, it is largely suppressed in the Higgs funnel region considered here, as shown in the centre panel of Fig. 3.

In SUSY, the sbottom-gluino exchange diagrams shown in Fig. 2 give rise to additional corrections at $\mathcal{O}(\alpha_s)$. The self-energy diagram leads to the mass renormalization [8]

$$\Delta m_b = \frac{\alpha_s(s) C_F}{\pi} \frac{m_{\tilde{g}}}{2} (A_b - \mu \tan \beta) I(m_{b_1}^2, m_{b_2}^2, m_{\tilde{g}}^2) \quad (9)$$

where $I(m_1, m_2, m_3) = C_0(0, 0, 0; m_1, m_2, m_3)$ is the 3-point function at zero external momentum. In this low-energy (LE) limit, and neglecting A_b with respect to the $\tan\beta$ -enhanced μ , the vertex correction equals the mass renormalization [16] up to a factor $1/\tan^2\beta$, so that the total SUSY correction becomes

$$\Delta_{\text{SUSY}}^{(\text{LE})} = \frac{\alpha_s(s)C_F}{\pi} \frac{1 + \tan^2\beta}{\tan^2\beta} m_{\tilde{g}} \mu \tan\beta \times I(m_{\tilde{b}_1}, m_{\tilde{b}_2}, m_{\tilde{g}}). \quad (10)$$

As A_b may be of similar size as $\mu \tan\beta$, its contribution must also be resummed. This is effectively done by replacing [17]

$$\lim_{A_b \rightarrow 0} \Delta m_b \rightarrow \frac{\lim_{A_b \rightarrow 0} \Delta m_b}{1 + \lim_{\mu \tan\beta \rightarrow 0} \Delta m_b}. \quad (11)$$

Finally, our result agrees with the those in Refs. [18], and we implement the finite $\mathcal{O}(m_b, s, 1/\tan^2\beta)$ remainder as described in Ref. [17].

3 Numerical discussion

For our numerical study of the impact of the QCD, top-quark loop, and SUSY-QCD corrections discussed above, we place ourselves in a minimal supergravity (mSUGRA) scenario with five parameters m_0 , $m_{1/2}$, $A_0 = 0$, $\tan\beta$, and $\text{sgn}(\mu)$ at the grand unification (GUT) scale. The weak-scale MSSM parameters are then determined through renormalization group running using `SPheno` [19], and the physical Higgs and SUSY masses with `FeynHiggs` [20]. For the SM inputs, i.e. masses and widths of the and electroweak gauge bosons and quarks, the coupling constants, the entries of the CKM-matrix, and the CP -violating phase, we refer the reader to Ref. [21].

We first study the effect of the corrections on the annihilation cross section relative to the process $\chi\chi \rightarrow A^0 \rightarrow b\bar{b}$, which is presented in the left-hand panel of Fig. 3. The corrected cross section σ_{NLO} is shown normalized to the leading order (LO) cross section σ_{LO} , including either only the QCD diagrams, QCD and top-loop diagrams, or the full SUSY-QCD correction. The QCD correction is independent of the SUSY parameters, while the top-quark loop correction is proportional to $1/\tan^2\beta$ through the $A^0 t\bar{t}$ coupling. The points, for which the SUSY-QCD corrections are evaluated, lie within the Higgs-funnel region and are indicated by a point in the left and centre panels of Fig. 4, for $\mu < 0$ and $\mu > 0$, respectively. It becomes clear that the annihilation cross section is decreased by about a factor two by the QCD contribution, where the principal contribution comes from the mass shift $m_b \rightarrow \bar{m}_b(s)$. The top-quark loop contribution, as already mentioned, is negligible with respect to the QCD contribution at large $\tan\beta$ such as in the A -funnel region. In the centre panel of Fig. 3 we see that Δ_{top} accounts for a few permille with respect to Δ_{QCD} for $\tan\beta \simeq 2$, and only for less than 10^{-5} for $\tan\beta > 40$.

When adding the SUSY-QCD contribution Δ_{SUSY} , the annihilation cross section receives another important correction, see left-hand panel of Fig. 3. The SUSY correction decreases the cross section by another few percent at very low $\tan\beta$ and up to another 40 (10) percent for $\mu < 0$ ($\mu > 0$), which underlines the importance of the full correction in the cosmological A -funnel region. The large difference between the correction factors for $\mu > 0$ and $\mu < 0$ is mainly due to the mass renormalization, Eq. (9), that is directly affected by $\text{sgn}(\mu)$.

To evaluate the effect of the corrections on the cold dark matter relic density, we have implemented our full SUSY-QCD correction, as described above, into the `DarkSUSY` package [6], which includes by default only the QCD corrections up to order $\mathcal{O}(\alpha_s^2)$ without their dependence on the energy scale s . Choosing either the pure Born or full SUSY-QCD calculation of the process $\chi\chi \rightarrow A^0 \rightarrow b\bar{b}$, we compare the resulting cold dark matter relic density $\Omega_{\text{CDM}} h^2$ to the observational 2σ range in Eq. (1) to determine the favoured regions in the $m_0 - m_{1/2}$ plane shown in the left-hand and centre panels of Fig. 4. As expected, the corrections do not affect the cosmological focus point (very low $m_{1/2}$), bulk (low m_0 and $m_{1/2}$) and coannihilation (low m_0) regions, where the inspected process is suppressed with respect to other (co)annihilation channels. However, at large $\tan\beta = 44.5$ (54) for $\mu < 0$ ($\mu > 0$), which still allow for electroweak symmetry breaking (EWSB) in a large region of the scanned $m_0 - m_{1/2}$ plane, the LO allowed regions (light) are dramatically changed by the full SUSY corrections (dark), which reduce σ_{eff} as discussed above. The increase in Ω_{CDM} is compensated by a shift towards smaller SUSY masses.

In the right-hand panel of Fig. 3 we plot the relic density for $m_0 = 1200$ GeV as function of $m_{1/2}$. The graph shows the contributions of the different correction terms. The effect of the $\mathcal{O}(\alpha_s^2)$ QCD corrections already included in `DarkSUSY` is considerably enhanced by our newly included $\mathcal{O}(\alpha_s^3)$ QCD and $\mathcal{O}(\alpha_s)$ SUSY-QCD corrections. Interesting effects due to the simultaneous correction of the Higgs decay width Γ_A are observed, e.g. the minimum of Ω_{CDM} is shifted towards the resonance $2m_\chi = m_A$. For a detailed discussion the reader is referred to Ref. [11].

Finally we note a difference between the relic density calculated with our code based on `SPheno` and `FeynHiggs` with respect to the one based on `ISAJET`, which is by default included in the `DarkSUSY` package. The right-hand panel of Fig. 4 shows the A -funnel region for $\mu < 0$, which is to be found at smaller values of m_0 . This difference should be due to the fact that the spectrum calculation is especially sensible to the spectrum generator for the neutralino and Higgs boson masses. In consequence, the resonance condition $2m_\chi = m_A$, governing the A -funnel region, can be shifted in an important way. However, the effect of the SUSY-QCD corrections is the same, i.e. an important shift of the favoured region with respect to a leading order result. For more details on the impact of SUSY

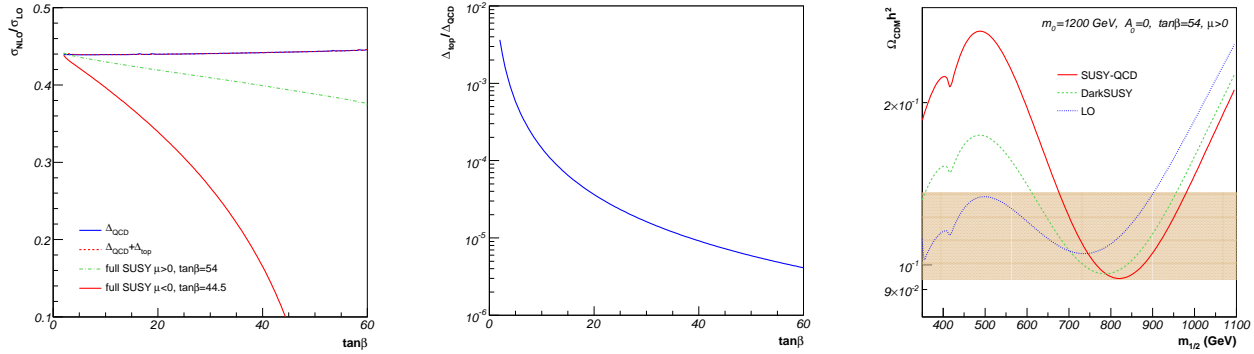


Fig. 3. Left and centre: NLO annihilation cross section in units of the LO cross section, including the QCD, QCD and top, and the full SUSY-QCD correction and ratio of top-quark loop correction and QCD correction as function of $\tan\beta$. Right: Dark matter relic density based on LO, NLO QCD, and full NLO SUSY-QCD calculation as function of $m_{1/2}$ for $m_0 = 1200$ GeV, $\mu < 0$, $\tan\beta = 44.5$ (slope indicated in the left panel of Fig. 4).

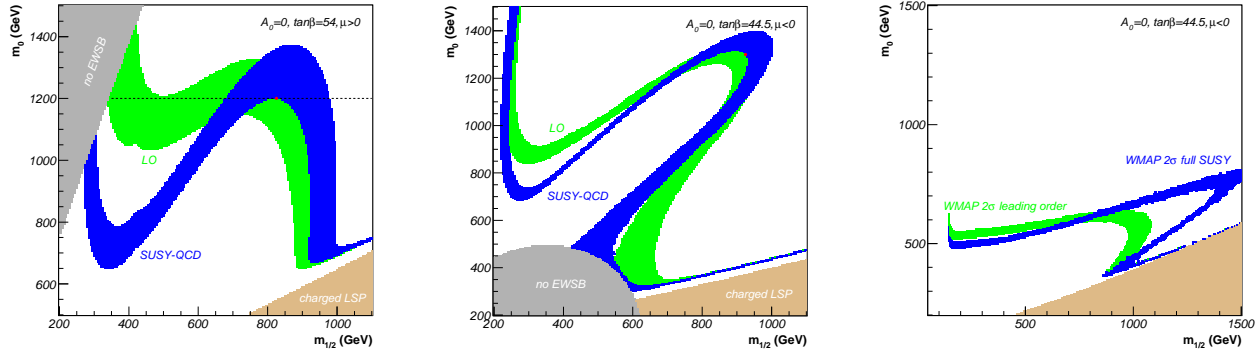


Fig. 4. Regions in the mSUGRA $m_0 - m_{1/2}$ plane forbidden by a charged LSP / no EWSB and favoured by the observed cold dark matter relic density $\Omega_{\text{CDM}} h^2$ including LO (light) and full SUSY-QCD (dark) calculation. The corresponding SUSY spectrum has been obtained using SPheno / FeynHiggs for the left and centre panels, and using ISAJET for the right panel.

spectrum calculations on dark matter annihilation see Ref. [22].

4 Conclusion

We have presented a complete calculation of SUSY-QCD corrections to dark matter annihilation in the Higgs-funnel, resumming potentially large $\mu \tan\beta$ and A_b contributions. We have demonstrated numerically that these corrections strongly influence the extraction of SUSY parameters from cosmological data and must therefore be included in common analysis tools like DarkSUSY or micrOMEGAS.

References

1. D. Spergel *et al.* [WMAP collaboration], *Astrophys. J. Suppl.* **170** (2007) 377.
2. R. Massey *et al.*, *Nature* **445** (2007) 286; M. J. Lee *et al.*, *Astrophys. J.* **661** (2007) 278.
3. A. Hamann *et al.*, *Phys. Rev. D* **75** (2007) 023522.
4. G. Bertone *et al.*, *Phys. Rept.* **405** (2005) 279.
5. G. Jungman *et al.*, *Phys. Rept.* **267** (1996) 195.
6. P. Gondolo *et al.*, *JCAP* **0407** (2004) 008.
7. G. Bélanger *et al.*, *Comput. Phys. Commun.* **149** (2002) 103.
8. M. S. Carena *et al.*, *Nucl. Phys. B* **429** (1994) 269.
9. W. de Boer *et al.*, *Astron. Astrophys.* **444** (2005) 51; *Phys. Lett. B* **636** (2006) 13.
10. L. Bergstrom *et al.*, *JCAP* **0605** (2006) 006.
11. B. Herrmann and M. Klasen, arXiv:0709.0043 [hep-ph], submitted to PRL.
12. M. Drees *et al.*, *Phys. Rev. D* **41** (1990) 1547; *Phys. Lett. B* (1990) 455; [Erratum-ibid. B **262** (1991) 497].
13. E. Braaten *et al.*, *Phys. Rev. D* **22** (1980) 715.
14. K. G. Chetyrkin, *Phys. Lett. B* **390** (1997) 309.
15. K. G. Chetyrkin *et al.*, *Nucl. Phys. B* **461** (1996) 3.
16. M. S. Carena *et al.*, *Nucl. Phys. B* **577** (2000) 88.
17. J. Guasch *et al.*, *Phys. Rev. D* **68** (2003) 115001.
18. A. Dabelstein, *Nucl. Phys. B* **456** (1995) 25; J. A. Coarasa *et al.*, *Phys. Lett. B* **389** (1996) 312.
19. W. Porod, *Comput. Phys. Commun.* **153** (2003) 275.
20. S. Heinemeyer *et al.*, *Comput. Phys. Commun.* **124** (2000) 76.
21. W. M. Yao *et al.* [Particle Data Group], *J. Phys. G* **33** (2006) 1.
22. G. Bélanger *et al.*, *Phys. Rev. D* **72** (2005) 015003.